COMMUNICATION

Protein interactions of dirhodium tetraacetate: a structural study

Received 00th January 20xx,
Accepted 00th January 20xx

DOI: 10.1039/x0xx00000x

Giarita Ferraro,[a†] Alessandro Pratesi,[b†] Luigi Messori[a]* and Antonello Merlino[c]*

The interactions between the cytotoxic paddlewheel dirhodium complex $[Rh_2(\mu\text{-}O_2CCH_3)_4]$ and the model protein bovine pancreatic ribonuclease (RNase A) were investigated by high-resolution mass spectrometry and X-ray crystallography. Results indicate that $[Rh_2(\mu\text{-}O_2CCH_3)_4]$ extensively reacts with RNase A. The metal compound binds the protein via coordination of the imidazole ring of a His side chain to one of its axial site, while the dirhodium center and the acetato ligands remain unmodifed. Data provide valuable information for the design of artificial dirhodium-containing metalloenzymes.

Introduction

Dirhodium(II) complexes of general formula $[Rh_2(O_2CR)_4]L_2$ (R=CH_3-, CH_3CH_2-, etc.; L=solvent) contain a Rh(II)–Rh(II) unit (bond length = 2.39 Å), four bridging equatorial carboxylato ligands arranged in a lantern-like fashion around the metal centers, and two possible donor ligands (L) at the axial coordination sites. These molecules have attracted considerable attention from the scientific community[1-7], since they are efficient catalysts for a variety of important reactions[8-13], such as C–H insertion into aliphatic and aromatic C-H bonds, X-H insertion (X=N, O, S), aromatic cycloaddition, decomposition of ethyl diazoacetate[1], hydrosilylation of alkynes [11-12] and oxidation of alcohols[13].

The paddlewheel dirhodium tetracetate complex ($[Rh_2(\mu\text{-}O_2CCH_3)_4]$, Figure 1) has been also considered as a promising catalyst for photochemical hydrogen evolution[14] and as a potential anticancer compound, since it exhibits an appreciable carcinostatic activity, though lower than cisplatin[2-4, 15-17]. Analogous compounds were found to be effective against Ehrlich ascites [2-4, 15-17], L1210 tumors [6-7], sarcoma 180 and P388 leukemia[18], but the appearance of severe toxic side effects prevented their further evaluation. Although the origin of the antitumor activity of dirhodium carboxylates is not known, plausible cellular targets are single-stranded and double stranded DNA[18], amino acids[19-20], peptides[21-22] and proteins[23-29]. In this frame, though several studies on the interactions of $[Rh_2(\mu\text{-}O_2CCH_3)_4]$ with peptides and proteins have been reported in the literature[23-29], the mode of binding of the dirhodium center to proteins has not been elucidated yet.

The reaction of $[Rh_2(\mu\text{-}O_2CCH_3)_4]$ with glutathione, Cys and its derivatives produces Rh(III)-Rh(III) complexes and oligomeric species containing dinuclear Rh(III)-Rh(III) units (with a Rh….Rh distance of 3.1 Å)[20]. The interaction with a few peptides induces the formation of stable adducts where Asp or Glu side chains replace the acetate units[21-22]. A similar mode of binding, where Asp side chains replace the acetate ligands, was observed in the interaction of a diruthenium tetracetate compound with hen egg white lysozyme (HEWL)[30]. Binding of $[Rh_2(\mu\text{-}O_2CCH_3)_4]$ to human serum albumin occurs via metal compound decomposition, oxidation of Rh(II) to Rh(III) and binding of Rh(III) to His residues[26]. The reaction of $[Rh_2(\mu\text{-}O_2CCH_3)_4]$ with metallothionein leads to formation of adducts showing displacement of the acetato ligands and coordination of Cys residues to the dirhodium center[29].

Based on these arguments, we have investigated here the interaction of $[Rh_2(\mu\text{-}O_2CCH_3)_4]$ with the model protein bovine pancreatic ribonuclease (RNase A) from the structural point of view.

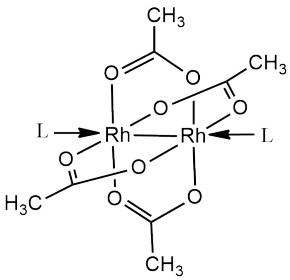

Figure 1. Typical paddle-wheel structure of $[Rh_2(\mu\text{-}O_2CCH_3)_4]$ unit. Axial donor ligands (L) are shown.

The reactivity of $[Rh_2(\mu\text{-}O_2CCH_3)_4]$ with RNase A has been first studied in solution by UV-vis absorption spectroscopy, circular dichroism and electrospray ionization mass spectrometry.

UV-vis absorption spectra of $[Rh_2(\mu\text{-}O_2CCH_3)_4]$ recorded in sodium citrate and ammonium acetate solutions indicate a different

[a] *Department of Chemistry "Ugo Schiff", University of Florence, via della Lastruccia, 3-13, 50019, Sesto Fiorentino, Florence, Italy. E-mail:luigi.messori@unifi.it*
[b] *Department of Chemistry and Industrial Chemistry, University of Pisa, Via Giuseppe Moruzzi 13, 56124, Pisa, Italy.*
[c] *Department of Chemical Sciences, University of Naples Federico II, Complesso Universitario di Monte Sant'Angelo, via Cinthia, 21, 80126, Naples, Italy. E-mail:antonello.merlino@unina.it*
† The authors equally contributed to this work.
Electronic Supplementary Information (ESI) available: [details of any supplementary information available should be included here]. See DOI: 10.1039/x0xx00000x

behaviour of $[Rh_2(\mu\text{-}O_2CCH_3)_4]$ in the absence and in the presence of the protein. In both solutions, in the absence of the protein, the spectral profile of the metallodrug shows two peaks in the visible region, at 448 and 586 nm and a shoulder at 340 nm. The band at 448 nm has been assigned to $Rh_2(\pi^*) \rightarrow Rh–O(\sigma^*)$ transitions of the tetraacetate ligands; the band at 586 nm has been assigned to $Rh_2(\pi^*) \rightarrow Rh_2(\sigma^*)$ transition of the metal–metal single bond. The spectra do not experience any change during 24 h (Figures S1A and S1B). This indicates that the compound is stable under the investigated solution conditions. On the contrary, in the presence of RNase A, the overall spectral profile is significantly different when compared to that reported in the absence of the protein (Figures S1B and S1C). There is a blue shift of λ_{max} from 448 nm to 442 nm and from 586 nm to 570 nm and the appearance of a new peak at 410 nm. The appearance of this new peak could be attributed to ligand-to-metal charge transfer band due to the coordination of a new ligand. The changes in λ_{max} clearly indicate that a reaction between the protein and the metal compound occurs. The blue shift of the $Rh_2(\pi^*) \rightarrow Rh–O(\sigma^*)$ transition band indicates that the protein binds the complex and that the Rh–Rh single bond is still intact after protein binding.

CD spectra of the protein incubated for 24 h with $[Rh_2(\mu\text{-}O_2CCH_3)_4]$ in 1:3 protein to metallodrug molar ratio are reported in Figure S2. CD spectra of RNase A in the presence of $[Rh_2(\mu\text{-}O_2CCH_3)_4]$ show a reduction of molar ellipticity, although the overall spectral features suggest that RNase A remains folded in the presence of the metal compound. Enzymatic activity studies offer further evidence that $[Rh_2(\mu\text{-}O_2CCH_3)_4]$ binds RNase A; indeed the dirhodium compound affects significantly the catalytic properties of the protein (Figure S3). Subsequently, electrospray ionization mass spectrometry (ESI MS) experiments were carried out at different time intervals after mixing (24 h, 48h, 72h), following a well-established protocol.[31,33] In Figure 2 the ESI mass spectrum recorded after 24h of incubation at 37 °C is reported (for the other incubation times and metal to protein ratios, see SI). From inspection of the spectrum it may be inferred that $[Rh_2(\mu\text{-}O_2CCH_3)_4]$ binds RNase A forming several Rh-protein adducts of different nature and stoichiometry. A summary of the metallic fragments that are found associated to the protein is reported in Table 1. RNase A binds $[Rh_2(\mu\text{-}O_2CCH_3)_4]$, naked Rh ions and a dirhodium centre with 2-4 Ac ligands. A large fraction of the protein remains unlabelled in the presence of the metal compound.

Notably, a complex pattern of adducts was previously reported for ESI MS spectra registered upon reacting $[Rh_2(\mu\text{-}O_2CCH_3)_4]$ with metallothionein[29].

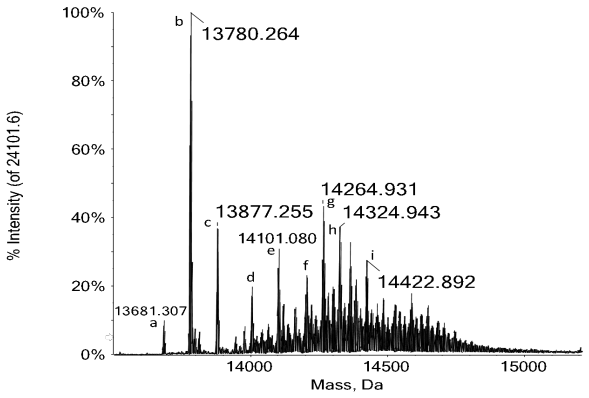

Figure 2. Deconvoluted ESI MS of RNase A (10^{-7} mol L^{-1}) treated with $[Rh_2(\mu\text{-}O_2CCH_3)_4]$ in a protein:metal ratio = 1:3 in 2×10^{-3} mol L^{-1} ammonium acetate solution at pH 6.8 and recorded after 24 h of incubation at 37 °C.

Table 1. ESI MS assignment.

Peak[a]	Mass, Da[a]	Adduct type
a	13681.307	RNase A
b	13780.246	RNase A+ sulfate/phosphate
c	13878.228	RNase A+ (sulfate/phosphate)$_2$
d	14003.102	RNase A+ $Rh_2(Ac)_2$
e	14101.080	RNase A+ $Rh_2(Ac)_2$ + sulfate/phosphate
f	14203.912	RNase A+Rh + $Rh_2(Ac)_2$ + sulfate/phosphate
g	14264.931	RNase A+Rh + $Rh_2(Ac)_3$ + sulfate/phosphate
h	14324.943	RNase A+Rh + $Rh_2(Ac)_4$ + sulfate/phosphate
i	14422.892	RNase A+2Rh + $Rh_2(Ac)_4$ + sulfate/phosphate

[a] Peaks in Table 1 refer to Figure 2. Ac=acetato ligand. The presence of sulfate/phosphate ions bound to $[Rh_2(\mu\text{-}O_2CCH_3)4]$/RNase A adducts is not surprising since these ions are bound to the commercial sample of the protein. Peaks of RNase A+ sulfate/phosphate ions are found also in the ESI MS spectra of the metal-free protein.

Afterward, the formation of $[Rh_2(\mu\text{-}O_2CCH_3)_4]$/RNase A adducts was investigated at solid state by X-ray crystallography. Crystals of $[Rh_2(\mu\text{-}O_2CCH_3)_4]$/RNase A adducts were obtained by soaking experiments: crystals of RNase A (space group C 1 2 1, with two protein molecules in the asymmetric unit) were grown by the hanging drop vapor diffusion method using a protein concentration of 20 mg mL^{-1} and a reservoir solution of 22% PEG4000 and 10 mM sodium citrate at pH 5.1, and then soaked for 7 days in a solution consisting of the reservoir at which the metal compound was added to a final concentration of 0.005 M. X-ray diffraction data on two distinct crystals were collected at 1.4 and 1.8 Å resolution at the XRD2 beamline of Elettra synchrotron in Trieste, Italy. Details of data collections and refinements are reported in Supporting info. The two structures are very similar to each other. The overall structure of the protein, reported in Figure 3, is not significantly affected by the interaction with the metal compound. Root mean square deviation of Cα atoms from the structure of the metal-free protein (PDB code 1JVT) is within the range as 0.38-0.58 Å. The most significant differences in the structure of RNase A upon reaction with $[Rh_2(\mu\text{-}O_2CCH_3)_4]$ are located close to the Rh binding sites, at level of the side chains of His105 and of His119 in both protein molecules present in the asymmetric unit. In both binding sites, the imidazole ring of the His side chain coordinates the dirhodium centre at the axial coordination site[34] (Figure 3). Close to His119 side chain, in the protein active site, the electron density maps are very well defined and unambiguously indicate that the compound retains the dimetallic centre and the acetato ligands upon protein binding (Figure 4A, Figures S4A, S5A and S5C). A water molecule occupies the remaining axial position. In molecule A, one acetate ion is not far from the side chain of Lys7, while the others are close to a number of solvent molecules. In molecule B, one acetato ligand and the axial water molecule are in contact with the Nζ atom of the side chain of Lys7, while another acetate is in contact with the Nζ atom of Lys91 of a symmetry related molecule. Close to the side chains of His105 of molecule A, electron density maps for the ligands are well defined

and in agreement with what observed in the protein active site (Figure 4B, Figures S4B and S5B). In molecule B the electron density maps are less well defined (Figure S4B), but in the second crystal it is not sufficiently well defined to assign Rh ligands (Figure S5D). This could suggest the possibility of a replacement of at least two acetate ligands with solvent molecules (Figure S5D).

Refinements point out that in the structure of the [Rh_2(μ-O_2CCH_3)$_4$]/RNase A adduct the Rh atoms have high occupancy (occupancy 0.6-0.7 and B-factors in the range 17—29 Å^2), indicating a relevant degree of protein metalation. Details on the dirhodium moiety geometry are reported in Table 2.

These structures represent a rare example of an adduct formed in the reaction of a protein with a Rh compound. A search in the Protein Data Bank reveals that there are only 7 proteins, whose structures have been solved in the presence of Rh compounds and that there are four examples of protein adducts with Rh atoms bound to the side chain of a His residue.

To provide an additional evidence of the relevance of adduct obtained by the crystallographic studies, crystals of the adducts have been dissolved and the catalytic activity of the obtained solution has been studied in comparison with that observed for a related solution obtained dissolving a similar amount of crystals of the native protein. This experiment confirms that the crystallographic adduct presents a catalytic activity significantly lower than that of the native protein. To verify if the binding of [Rh_2(μ-O_2CCH_3)$_4$] to imidazole occurs also in solution, under the experimental conditions used to grow protein crystals, UV-Vis absorption spectra of the compound upon titration with increasing amounts of imidazole were collected (Figure S6). A gradual shift of the band at 584 nm up to 566 nm, accompained by an increase in the absorbance of the shoulder at 353 nm, has been observed. This observation supports the binding of the dirhodium compound to the imidazole.

Axial binding to the dirhodium centre and replacement of the acetato ligands were previously found in the products of the reaction of [Rh_2(μ-O_2CCH_3)$_4$] with methionine, although in this case formation of monometallic Rh centres is also observed[20,34]. Z. Ball and coworkers proposed that a His residue coordinates at the axial position of the dirhodium centre in the rhodium(II) conjugates of the Lyn SH3 domain, but in this adduct two acetato ligands are replaced by the side chains of two Glu residue side chains[35].

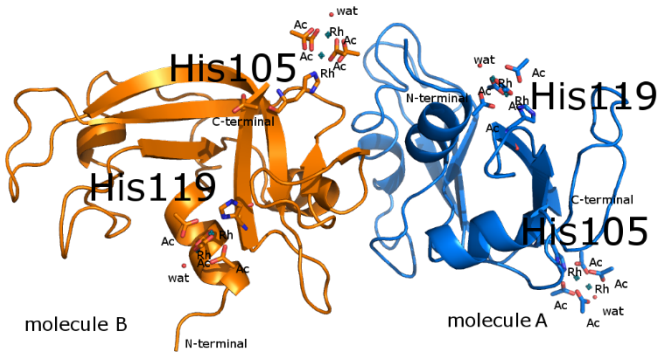

Figure 3. Overall structure of the two molecules in the asymmetric unit of the crystal of the adduct formed in the reaction of dirhodium tetraacetate with RNase A solved at 1.4 Å resolution. Rh atoms are in green.

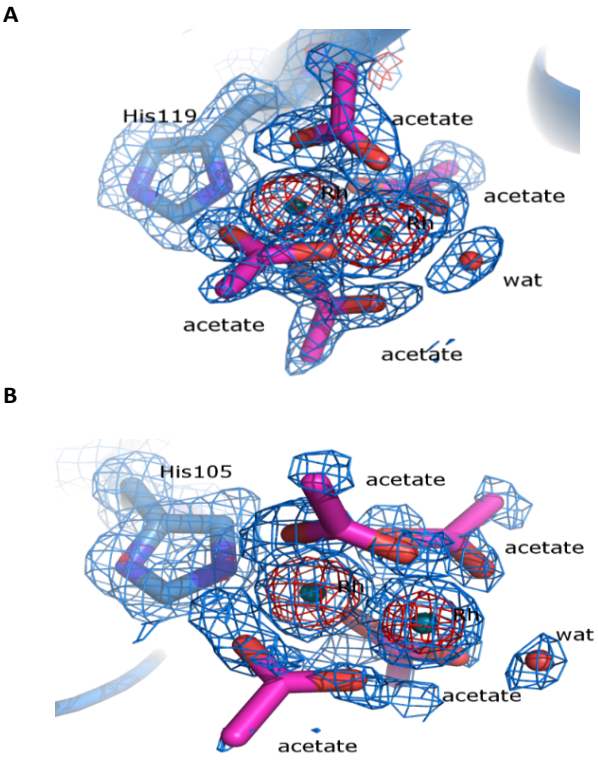

Figure 4. Details of the Rh binding sites in molecule A of the crystal of [Rh_2(μ-O_2CCH_3)$_4$]/RNase A adduct solved at 1.4 Å. The dirhodium center is retained and the side chains of His105 (A) or His119 (B) coordinate at the axial coordination site. 2Fo-Fc electron density maps are contoured at 5.0 σ (red) and 1.0 σ (blue).

Table 2. Selected bond lengths (Å) and angles (°) for the dirhodium centre coordinated to the side chains of His105 and His119, compared with the values observed in the crystal structure of the dirhodium tetracetate dihydrate[36].

	In the adduct				in Rh_2(μ-O_2CCH_3)$_4$[36]
	His119A	**His119B**	**His105A**	**His105B**	
Rh-Rh (Å)	2.34	2.37	2.42	2.42	2.39
Rh-$O_{(acetate)}$* (Å)	2.09	2.11	2.06	2.13	2.04
Rh-N (Å)	2.16	2.27	2.20	2.18	
Rh-O_{wat} (Å)	2.24	2.28	2.29	2.28	2.31
$O_{(ac)}$-Rh-$O_{(wat)}$* (°)	93.7	93.9	94.4	92.5	91.9 89.2<x<94.8
$O_{(ac)}$-Rh-N* (°)	90.9	91.9	91.1	93.3	
Rh-Rh-N (°)	177.1	175.4	176.3	176.6	
Rh-Rh-O* (°)	90.1	88.0	88.9	87.3	88.1 87.8<x<88.3

*average values. Standard deviations for the distances are in the range 0.04-0.14 Å. Standard deviations for the angles are in the range 2.5°-12.7°

In conclusion, we have analysed the interaction of [Rh_2(μ-O_2CCH_3)$_4$] with the model protein RNase A. Our combined crystallographic/spectrometric approach unambigously indicates that [Rh_2(μ-O_2CCH_3)$_4$] binds RNase A forming a variety of possibile

adducts. ESI MS data show that the protein binds $[Rh_2(\mu\text{-}O_2CCH_3)_4]$, naked Rh ions and dirhodium moieties with 2-4 Ac ligands. X-ray crystallography data show that the binding of the intact compound can occur through coordination of a His side chain to the axial site of the dirhodium complex. Although some differences are noticed when comparing the ESI MS and crystalographic data (which may be easily accounted for considering the different experimental conditions needed to perform the two experiments), the results demonstrate that upon protein binding dirhodium complexes can retain their dimetallic center, as observed in the case of diruthenium compounds[31], and their acetate ligands, contrarily to previous suggestions[31,35]. The $[Rh_2(\mu\text{-}O_2CCH_3)_4]$ binding does not alter the overall conformation of the enzyme (that remains well-folded), although it affects the catalytic properties of the protein.

These results help to understand the reactivity of dirhodium carboxylates with peptides and proteins, providing useful information for the design of new dirhodium/peptide and dirhodium/protein adducts with an array of potential applications ranging from catalysis to cancer treatment.

The authors thank Elettra staff for technical assistance. L.M. acknowledges Beneficentia Stiftung (Vaduz, Liechtenstein) and AIRC (IG-12085) for financial support. G. F. thanks AIRC foundation for her 3-years FIRC fellowship. A.P. acknowledges the University of Pisa (Rating Ateneo 2019) for financial support.

Notes and References

1 R. Paulissenen, H. Reimlinger, E. Hayez, A. J. Hubert and P. Teyssie. *Tetrahedron Lett.* 1973, **14**, 2233-2236.
2 A. Erck, L. Rainen, J. Whileyman, I.M. Chang, A. P. Kimball and J.L. Bear. *Proc. Soc. Exp. Biol. Med*. 1974, **145**, 1278-1283.
3 J. L. Bear, H. B. Jr. Gray, L. Rainen, I. M. Chang, R. Howard, G. Serio and A. P. Kimball. *Cancer Chemother. Rep*. 1975, **59**, 611-620.
4 I. Chang and W. S. Woo. *Korean Biochem. J.* 1976, **9**, 175-180.
5 R. A. Howard, E. Sherwood, A. Erck, A. P. Kimball and J. L. Bear. *J. Med. Chem.* 1977, **20**, 943-946.
6 R. G. Hughes, J. L. Bear and A. P. Kimball. *Am. Assoc. Cancer Res.* 1972, **13**, 120-120.
7 R. A. Howard, A. P. Kimball, and J. L. Bear. *Cancer Res.* 1979, **39**, 2568-2573.
8 M. P. Doyle. *J Org Chem.* 2006, **71**(25), 9253–9260.
9 H. M. L. Davies and R. E. Beckwith. *Chem. Rev*. 2003, **103**, 2861-2904.
10 M. P. Doyle. Catalytic Asymmetric Synthesis. 2nd ed., Chap. 5, ed.by Ojima 1., Wiley-VCR, New York, 2000, 191-228.
11 M. P. Doyle, K. G. High, C. L. Nesloney, T. W. Jr. Clayton and J. Lin. *Organometal*. 1991, **10**, 1225-1126.
12 M. P. Doyle, G. A. Devora, A. O. Nefedov and K. G. High. *Organometal* 1992, **11**, 549-555.
13 M. P. Doyle, J. W. Terpstra, C. H. Winter and J. H. Griffin. J. *Mol. Catal.* 1984, **26**, 259—266.
14 Y. Kataoka, N. Yano, M. Hand and T. Kawamoto. *Dalton Trans*. 2019, **48**(21), 7302-7312.
15 S. Zyngier, E. Kimura and R. Najjar. *Braz. J. Med. Biol. Res*. 1989, **22**, 397-401.
16 E. M. Reibscheid, S. Zyngier, D. A. Maria, R. J. Mistrone, R. D. Sinisterra, L. G. Couto and R. Najjar. *Braz. J. Med. Biol. Res.* 1994, **27**, 91-94.
17 M. S. Nothenberg, S. B. Zyngier, A. M. Giesbrecht, M. T. P. Gambardella, R. H. A. Santos, E. Kimura and R. Najjar. *J. Braz. Chem. Soc*. 1994, **5**, 23-29.
18 J. L. Bear. Rhodium compounds for antitumor use, in: Precious Met. Proc. Jnt. Precious Met. Inst, Conf., 9th, 1986, 337–344.
19 G. Szilvagyi, M. Hollosi, L. Tolgyesi, J. Frelek and Z. Majer. *Tetrahedron*. *Asymmetry* 2008, **19**, 2594-2599.
20 A. E. Garcia, F. Jalilehvand, P. Niksirat. *J synchrotron radiation* 2019, **26** (2); A. E. Garcia, F. Jalilehvand, P. Niksirat and B. S. Gelfand. *Inorg. Chem.* 2018, **57**, 12787-12799; F. Jalilehvand; A. Enriquez Garcia; P. Niksirat, ACS Omega 2017, 2, 6174 6186.
21 B. V. Popp, Z. Chen and Z. T. Ball. *Chem Commun* 2012, **48**, 7492-7494.
22 A. N. Zaykov and Z. T. Ball. *Chem Commun* 2011, **47**, 10927-10929.
23 R. A. Howard, T. G. Spring and J. L. Bear. *Cancer Res*. 1976, **36**, 4402-4405.
24 K. Sorasaenee, P. K.-L. Fu, A. M. Angeles-Boza, K. R. Dunbar and C. Turro. *Inorg. Chem.* 2003, **42**, 1267-1271.
25 H. T. Chifotides, P. K.-L. Fu, K. R. Dunbar and C. Turro. *Inorg. Chem*. 2004, **43**, 1175-1183.
26 L. Trynda and F. Pruchnik. *J. Inorg. Biochem.* 1995, **58**, 69-77.
27 B. P. Esposito, E. de Oliveira, S. B. Zyngier and R. Najjar. *J. Braz. Chem. Soc*. 2000, **11**, 447-452.
28 J. Chen and M. Kostic. *Inorg. Chem.* 1988, **27**, 2682-2687.
29 D. L. Wongand and M. J. Stillman. *ACS OMEGA* 2018, **3**, 16314-16327.
30 L. Messori, T. Marzo, R. N. Fernandes Sanches, H.-U.-Rehman, D. de Oliveira Silva and A. Merlino. *Angewandte Chemie Int. Ed.* 2014, 10, **53**(24), 6172-6175.
31 E. Michelucci, G. Pieraccini, G. Moneti, C. Gabbiani, A. Pratesi and L. Messori. *Talanta*, 2017, **167**, 30-38.
32 A. Pratesi, D. Cirri, D. Fregona, G. Ferraro, A. Giorgio, A. Merlino and L. Messori. *Inorg. Chem.*, 2019, **58**, 10616-10619.
33 A. Pratesi, D. Cirri, L. Ciofi and L. Messori. *Inorg. Chem.*, 2018, **57**, 10507-10510.
34 R. Głaszczka. J Jaźwiński, B. Kamieński and M. Kamińska, *Tetrahedron. Asymmetry* 2010, **21**(19), 2346-2355.
35 F. Vohidov, S. E. Knudsen, P. G. Leonard, J. Ohata, M. J. Wheadon, B. V. Popp, J- E. Ladbury and Z. T. Ball. *Chem. Sci*. 2015, **6**, 4778-4783.
36 F. A. Cotton, B. G. Deboer, M. D. Laprade, J. R. Pipal and D. A. Ucko. *Acta Cryst. B* 1971, **27**, 1664-1671.

